

Nonlinear magneto-optical rotation in optically thick media

S. M. Rochester¹ and D. Budker^{1,2,*}

¹*Department of Physics, University of California at Berkeley, Berkeley, California 94720-7300*

²*Nuclear Science Division, Lawrence Berkeley National Laboratory, Berkeley, California 94720*

(Dated: October 24, 2018)

Nonlinear magneto-optical rotation is a sensitive technique for measuring magnetic fields. Here, the shot-noise-limited magnetometric sensitivity is analyzed for the case of optically-thick media and high light power, which has been the subject of recent experimental and theoretical investigations.

PACS numbers: 33.55.Ad,07.55.Ge

I. INTRODUCTION

Resonant nonlinear magneto-optical rotation (NMOR) [1, 2] has been the subject of extensive theoretical and experimental studies because it provides a very sensitive way to measure magnetic fields (see, e.g., Ref. [3]). While NMOR experiments are usually carried out with vapor samples of moderate optical thickness (no more than ~ 2 absorption lengths), the intense research of recent years on electromagnetically-induced transparency (EIT; see, e.g., Ref. [4] for a review) has motivated investigation of optically thick media [5, 6].

Recently, NMOR in the vicinity of the D1 and D2 lines by an optically thick vapor of rubidium was studied [7, 8, 9, 10, 11]. The authors of Ref. [8] used a 5 cm-long vapor cell containing ⁸⁷Rb and a laser beam tuned to the maximum of the NMOR spectrum near the D1 line (laser power was 2.5 mW, beam diameter ~ 2 mm). They measured maximum (with respect to laser frequency and magnetic field) polarization rotation φ_{max} as a function of atomic density. It was found that φ_{max} increases essentially linearly up to $n \approx 3.5 \times 10^{12} \text{ cm}^{-3}$. At higher densities, $d\varphi_{max}/dn$ decreases and eventually becomes negative. The maximum observed rotation was ≈ 10 rad with the applied magnetic field of ≈ 0.6 G. (This shows the effect of power broadening on the magnetic field dependence; at low light power, the maximum rotation would occur at a magnetic field about an order of magnitude smaller.) Rotation slope $d\varphi/dB|_{B=0}$, an important parameter for magnetometry, was also measured as a function of atomic density in Ref. [8].

The goal of the present contribution is to analyze the scaling of optimal magnetometric sensitivity with respect to optical thickness of the sample. We analyze NMOR for a simple system—an isolated $J = 1 \rightarrow J = 0$ transition—for which analytical solutions for the density matrix are readily obtained. We assume that the transverse thickness of the sample is small, so that the trapping of spontaneously-emitted radiation can be neglected. (This assumption may not be justified in actual experiments with optically thick media [9].) We also neglect mix-

ing between different velocity groups due to velocity-changing collisions. Such mixing is important in the presence of a buffer gas, or for anti-relaxation-coated cells.

A theoretical treatment of NMOR in dense media has been carried out earlier in Refs. [7] and [12]. The present analysis partially overlaps with this earlier work and extends it in several ways: we extend the treatment to the case of large Doppler broadening and the intermediate regime where power and Doppler widths are comparable; provide a qualitative discussion of the contribution to optical rotation as a function of optical depth in the medium; discuss the role of the coherence and the alignment-to-orientation conversion effects [13]; discuss scaling of magnetometric sensitivity with optical thickness of the medium; and finally, give a general argument on scaling based on the observation that an optimized nonlinear optical rotation measurement is a way to carry out a spin measurement of an atomic ensemble with sensitivity given by fundamental quantum noise limits [3, 12].

II. DESCRIPTION OF THE DENSITY MATRIX CALCULATION

The calculation is based on a standard density matrix approach. The time evolution of the atomic density matrix ρ is given by the Liouville equation (see, e.g., Ref. [14]):

$$\frac{d\rho}{dt} = \frac{1}{i\hbar}[H, \rho] - \frac{1}{2}\{\Gamma, \rho\} + \Lambda, \quad (1)$$

where the square brackets denote the commutator and the curly brackets the anti-commutator, and the total Hamiltonian H is the sum of light-atom interaction Hamiltonian $H_L = -\vec{d} \cdot \vec{E}$ (where \vec{E} is the electric field vector, and \vec{d} is the electric dipole operator), the magnetic field-atom interaction Hamiltonian $H_B = -\vec{\mu} \cdot \vec{B}$ (where \vec{B} is the magnetic field and $\vec{\mu}$ is the magnetic moment), and the unperturbed Hamiltonian H_0 . Γ is the relaxation matrix (diagonal in the collision-free approximation)

$$\langle \xi J m | \Gamma | \xi J m \rangle = \gamma + \gamma_0 \delta(\xi, \xi_e), \quad (2)$$

where γ is the ground state depolarization rate (e.g., due to transit of atoms through the laser beam), γ_0 is the

*Electronic address: budker@socrates.berkeley.edu

spontaneous decay rate from the upper state, and ξ represents the quantum number distinguishing the ground state (ξ_g) from the excited state (ξ_e). $\Lambda = \Lambda^0 + \Lambda^{repop}$ is the pumping term, where the diagonal matrix

$$\langle \xi_g J_g m | \Lambda^0 | \xi_g J_g m \rangle = \frac{\gamma \rho_0}{(2J_g + 1)} \quad (3)$$

describes incoherent ground state pumping (ρ_0 is the atomic density), and

$$\langle \xi_g J_g m | \Lambda^{repop} | \xi_g J_g m' \rangle = \gamma_0 \sum_{m_e, m'_e, q} \langle J_g, m, 1, q | J_e, m_e \rangle \langle J_g, m', 1, q | J_e, m'_e \rangle \rho_{\xi_e J_e m_e \xi_e J_e m'_e}, \quad (4)$$

describes repopulation due to spontaneous relaxation from the upper level (see, e.g., Ref. [15]). Here $\langle \dots | \dots \rangle$ are the Clebsch-Gordan coefficients.

The electric field vector is written (see, e.g., Ref. [16])

$$\begin{aligned} \vec{E} = & \frac{1}{2} \left[E_0 e^{i\phi} (\cos \varphi \cos \epsilon - i \sin \varphi \sin \epsilon) e^{i(\omega t - kz)} + c.c. \right] \hat{x} \\ & + \frac{1}{2} \left[E_0 e^{i\phi} (\sin \varphi \cos \epsilon + i \cos \varphi \sin \epsilon) e^{i(\omega t - kz)} + c.c. \right] \hat{y}, \end{aligned} \quad (5)$$

where ω is the light frequency, $k = \omega/c$ is the vacuum wave number, E_0 is the electric field amplitude, φ is the polarization angle, ϵ is the ellipticity (arctangent of the ratio of the major and minor axes of the polarization ellipse), and ϕ is the overall phase. By substituting (5) into the wave equation

$$\left(\frac{\omega^2}{c^2} + \frac{d^2}{dz^2} \right) \vec{E} = -\frac{4\pi}{c^2} \frac{d^2}{dt^2} \vec{P}, \quad (6)$$

where $\vec{P} = Tr(\rho \vec{d})$ is the polarization of the medium, the absorption, rotation, phase shift, and change of ellipticity per unit distance for an optically thin medium can be found in terms of the density matrix elements (these expressions are given in Ref. [17]). Once the solutions for the density matrix are obtained, we will perform an integration to generalize the result to media of arbitrary thickness.

III. THE DOPPLER-FREE CASE

We consider the case of a $J = 1 \rightarrow J = 0$ transition, and linearly-polarized incident light, with a magnetic field directed along the light propagation direction (Faraday geometry). Using the rotating wave approximation, the solution of Eq. (1) is obtained, and from this, analytic expressions for thin medium absorption and rotation are found. These expressions can be simplified by assuming that $\gamma \ll \gamma_0$. We first consider the case where the power-broadened line width is much greater than the

Doppler width. In this case, the absorption coefficient per unit length α is found to be

$$\alpha \approx \frac{\alpha_0}{(2\Delta/\gamma_0)^2 + 2\kappa/3 + 1}, \quad (7)$$

where Δ is the light-frequency detuning from resonance,

$$\kappa = \frac{d^2 E_0^2}{\hbar^2 \gamma \gamma_0} \quad (8)$$

is the optical pumping saturation parameter, and

$$\alpha_0 \approx \frac{1}{6\pi} \lambda^2 n \quad (9)$$

is the unsaturated absorption coefficient on resonance, where λ is the transition wavelength and n is the atomic density. For $\Omega \ll \gamma$, where $\Omega = g\mu B$ is the Larmor frequency (g is the Landé factor, and μ is the Bohr magneton), the slope of optical rotation per unit length, $d\varphi/(d\Omega dx)$, (proportional to rotation for small magnetic fields) is found to be

$$\frac{d\varphi}{d\Omega dx} \approx \frac{1}{\gamma} \frac{\alpha_0}{(2\Delta/\gamma_0)^2 + 2\kappa/3}, \quad (10)$$

where we have neglected linear optical rotation. In general, optical rotation can be induced by either linear dichroism or circular birefringence. Analysis of the steady-state polarization of the ground state shows that both processes contribute here: the contribution due to linear dichroism induced in the medium is given by

$$\left. \frac{d\varphi}{d\Omega dx} \right|_{dichr.} \approx \frac{1}{\gamma} \frac{1}{1 + (2\Delta/\gamma_0)^2} \frac{\alpha_0}{(2\Delta/\gamma_0)^2 + 2\kappa/3}, \quad (11)$$

and the contribution due to circular birefringence (arising due to alignment-to-orientation conversion in the presence of both the magnetic field and the strong electric field of the light [13]) is given by

$$\left. \frac{d\varphi}{d\Omega dx} \right|_{biref.} \approx \frac{1}{\gamma} \frac{(2\Delta/\gamma_0)^2}{1 + (2\Delta/\gamma_0)^2} \frac{\alpha_0}{(2\Delta/\gamma_0)^2 + 2\kappa/3}. \quad (12)$$

The sum of the two contributions produces the Lorentzian line shape of Eq. (10).

We now generalize the formulas for absorption and rotation to the case of thick media, and find the magnetometric sensitivity. In the Doppler-free case we are presently considering, we can further simplify the expressions by assuming $\Delta = 0$ (we will have to include non-zero detunings in the discussion of the Doppler-broadened case below), and $\kappa \gg 1$. (We will see from the final result that this holds everywhere in the medium when the input light power is optimal.) Generally, the medium in the presence of a magnetic field produces light ellipticity as well as rotation; however, the ellipticity is an odd function of detuning and is zero on resonance. The rate of change of the saturation parameter as light travels through the medium is given by

$$\begin{aligned} \frac{d\kappa(x)}{dx} &= -\alpha\kappa(x) \\ &\approx -\frac{3}{2}\alpha_0, \end{aligned} \quad (13)$$

so solving for the saturation parameter as a function of position,

$$\kappa(x) \approx \kappa_0 - \frac{3}{2}\alpha_0 x, \quad (14)$$

where κ_0 is the saturation parameter at $x = 0$.

The contribution to the small-field optical rotation of the “slice” of the medium at position x is found by substituting Eq. (14) into Eq. (10):

$$\frac{d\varphi}{d\Omega dx}(x) \approx \frac{1}{\gamma} \frac{\alpha_0}{2\kappa_0/3 - \alpha_0 x}. \quad (15)$$

This contribution is plotted as a function of position in Fig. 1. The plot illustrates that the part of the medium near its end contributes significantly more to the overall rotation than the part near its beginning. This is because light power, and correspondingly, the light broadening of the resonance, is lower at the end of the medium [the ratio of the rotation per unit length is approximately $\kappa(\ell)/\kappa_0 \approx 1 - (3/2)\alpha_0\ell/\kappa_0$]. Integrating over the length ℓ of the medium gives the total slope:

$$\begin{aligned} \frac{d\varphi}{d\Omega} &= \int_0^\ell \frac{d\varphi}{d\Omega dx}(x) dx \\ &\approx \frac{1}{\gamma} \int_0^\ell \frac{\alpha_0}{2\kappa_0/3 - \alpha_0 x} dx \\ &= \frac{1}{\gamma} \ln \left(\frac{\kappa_0}{\kappa_0 - 3\alpha_0\ell/2} \right). \end{aligned} \quad (16)$$

The slope (16) is plotted as a function of $\alpha_0\ell$ in Fig. 2.

The photon shot-noise-limited magnetometric sensitivity δB [22] is given in terms of the number N_γ of transmitted photons per unit time, the slope of rotation with

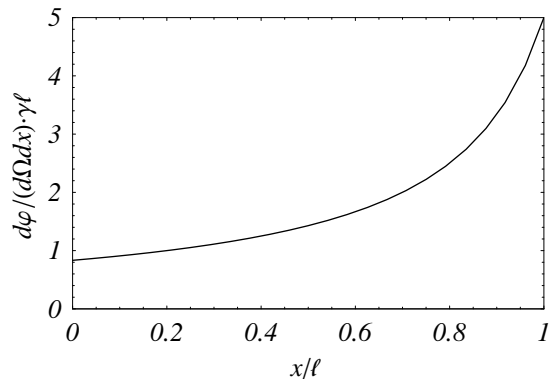


FIG. 1: Normalized contribution to small-field slope (in radians) of a slice of the medium of width dx at position x , given by Eq. 15. We have set $\kappa_0 = 1.8\alpha_0\ell$, the value which is later seen to produce the greatest magnetometric sensitivity.

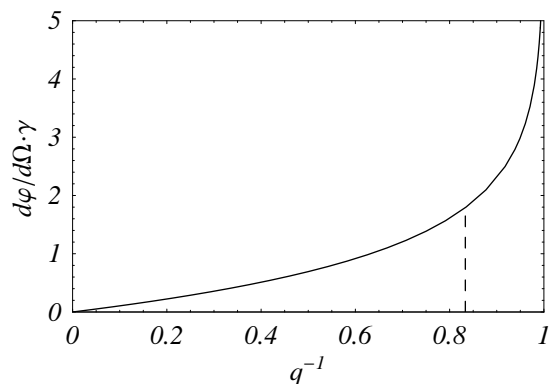


FIG. 2: Normalized slope (in radians) of NMOR as a function of optical thickness of the medium [$q^{-1} = (3/2)\alpha_0\ell/\kappa_0$]. The value of q^{-1} that produces the greatest magnetometric sensitivity is shown with a dashed line.

respect to B , and the measurement time t :

$$\begin{aligned} (\delta B)^{-1} &= 2 \frac{d\varphi}{dB} \sqrt{N_\gamma t} \\ &= \frac{g\mu\omega}{\hbar c} \frac{d\varphi}{d\Omega} \sqrt{\frac{2At}{\pi} \gamma \kappa(\ell)} \\ &\approx \frac{g\mu\omega}{\hbar c} \sqrt{\frac{2At}{\pi} \frac{\kappa_0 - \frac{3}{2}\alpha_0\ell}{\gamma}} \ln \left(\frac{\kappa_0}{\kappa_0 - 3\alpha_0\ell/2} \right) \\ &= \frac{g\mu\omega}{\hbar c} \sqrt{\frac{3}{\pi} \frac{At\alpha_0\ell}{\gamma}} \sqrt{q-1} \ln \left(\frac{q}{q-1} \right), \end{aligned} \quad (17)$$

where A is the cross-sectional area of the light beam and we have made the change of variables $\kappa_0 = 3q\alpha_0\ell/2$. The factor

$$\sqrt{q-1} \ln \left(\frac{q}{q-1} \right)$$

reaches a maximum of ~ 0.8 at $q \approx 1.2$ so we see that for media of sufficient thickness, i.e. where $\alpha_0\ell \gg 3$, and for

the optimum initial saturation parameter $\kappa_0 \approx 1.8\alpha_0\ell$, we have from Eq. (14) that $\kappa(x) \gg 1$ for all x . For the optimum light intensity, then,

$$\begin{aligned} (\delta B)^{-1} &\approx 0.8 \frac{g\mu\omega}{\hbar c} \sqrt{\frac{At\alpha_0\ell}{\gamma}} \\ &\approx 1.1 \frac{g\mu}{\hbar} \sqrt{\frac{A\ell nt}{\gamma}}. \end{aligned} \quad (18)$$

This result is consistent with the general observation [3] that optimized NMOR provides a method for measuring a spin-system at the standard quantum limit (SQL) given by spin-projection noise [23]. The sensitivity is then expected to scale as the square root of the product of the number of available atoms and the spin-relaxation time (see, e.g., Ref. [18], Sec. 3.1.1), which is indeed the result (18).

IV. THE DOPPLER-BROADENED CASE

Now we consider the case where the Doppler width Γ is much greater than the power-broadened line width. In this case, we need to average over the over the atomic velocity distribution, which is equivalent to averaging over the Doppler-free spectral profiles. On resonance with the Doppler broadened transition, the absorption coefficient is given by

$$\begin{aligned} \alpha_{DB} &\approx \frac{1}{\sqrt{\pi}\Gamma} \int_{-\infty}^{\infty} \alpha(\Delta) d\Delta \\ &\approx \frac{\alpha_0}{\sqrt{\pi}\Gamma} \int_{-\infty}^{\infty} \frac{d\Delta}{(2\Delta/\gamma_0)^2 + 2\kappa/3} \\ &= \sqrt{\frac{3\pi}{8}} \frac{\gamma_0}{\Gamma} \frac{\alpha_0}{\sqrt{\kappa}}. \end{aligned} \quad (19)$$

In this case the Doppler-broadened unsaturated absorption coefficient is given in terms of the Doppler-free unsaturated absorption coefficient by

$$\alpha_0|_{DB} = \frac{\sqrt{\pi}}{2} \frac{\gamma_0}{\Gamma} \alpha_0. \quad (20)$$

Comparing Eqs. (19) and (7), we see that we have reproduced a well-known result (see, e.g., Ref. [19], Sec. 7.2.1) that resonant absorption falls as $1/\kappa$ for Doppler-free media and as $1/\sqrt{\kappa}$ for Doppler-broadened media when $\kappa \gg 1$. The change in κ per unit length is

$$\begin{aligned} \frac{d\kappa(x)}{dx} &= -\alpha_{DB}\kappa(x) \\ &\approx -\frac{\sqrt{6\pi}}{4} \frac{\gamma_0}{\Gamma} \alpha_0 \sqrt{\kappa(x)}, \end{aligned} \quad (21)$$

and solving for κ as a function of position,

$$\kappa(x) \approx \left(\sqrt{\kappa_0} - \frac{\sqrt{6\pi}}{8} \frac{\gamma_0}{\Gamma} \alpha_0 x \right)^2. \quad (22)$$

Note that the behavior of the saturation parameter as a function of distance is different in the Doppler-broadened case compared to the Doppler-free case [cf. Eq. (14)] where the saturation parameter falls approximately linearly with distance.

Taking the average of small-field rotation over the Doppler distribution gives

$$\begin{aligned} \left. \frac{d\varphi}{d\Omega dx} \right|_{DB} &\approx \frac{1}{\sqrt{\pi}\Gamma} \int_{-\infty}^{\infty} \frac{d\varphi}{d\Omega dx}(\Delta) d\Delta \\ &\approx \frac{\alpha_0}{\sqrt{\pi}\Gamma} \int_{-\infty}^{\infty} \frac{1}{(2\Delta/\gamma_0)^2 + 2\kappa/3} d\Delta \\ &\approx \frac{\sqrt{6\pi}}{4} \frac{\gamma_0}{\Gamma} \frac{\alpha_0}{\gamma\sqrt{\kappa}}. \end{aligned} \quad (23)$$

We see that the rotation per unit length scales as $1/\sqrt{\kappa}$, in contrast to the $1/\kappa$ scaling for the Doppler-free case [similar to the situation with absorption, Eqs. (7,19)]. This is because the number of atoms producing the effect is, in a sense, not fixed; with increasing light power, a larger fraction of the Doppler distribution is involved.

Substituting (22) into Eq. (23) to find the contribution to the slope as a function of position gives

$$\left. \frac{d\varphi}{d\Omega dx}(x) \right|_{DB} \approx \frac{2}{\gamma} \frac{\alpha_0}{\frac{8}{\sqrt{6\pi}} \frac{\Gamma}{\gamma_0} \sqrt{\kappa_0} - \alpha_0 x}. \quad (24)$$

It is interesting to note that while the light power and the rotation slope per unit length behave differently in the Doppler-broadened case compared to the Doppler-free case, Eq. (24) has the same functional form as for the Doppler-free case [Eq. (15)].

Integrating over the length of the medium, we obtain

$$\begin{aligned} \left. \frac{d\varphi}{d\Omega} \right|_{DB} &\approx \int_0^\ell \left. \frac{d\varphi}{d\Omega dx}(x) \right|_{DB} dx \\ &\approx \frac{2}{\gamma} \int_0^\ell \frac{\alpha_0}{\frac{8}{\sqrt{6\pi}} \frac{\Gamma}{\gamma_0} \sqrt{\kappa_0} - \alpha_0 x} dx \\ &= \frac{2}{\gamma} \ln \left(\frac{\sqrt{\kappa_0}}{\sqrt{\kappa_0} - \frac{\sqrt{6\pi}}{8} \frac{\gamma_0}{\Gamma} \alpha_0 \ell} \right). \end{aligned} \quad (25)$$

The behavior of (25) as a function of $\alpha_0\ell$ is qualitatively similar to that of Eq. (16) shown in Fig. 2. However, the dependence on κ_0 is different.

The magnetometric sensitivity is given by

$$\begin{aligned} (\delta B)_{DB}^{-1} &= \frac{g\mu\omega}{\hbar c} \left. \frac{d\varphi}{d\Omega} \right|_{DB} \sqrt{\frac{2At}{\pi}} \gamma\kappa(\ell) \\ &\approx \frac{g\mu\omega}{\hbar c} \sqrt{\frac{8At}{\pi\gamma}} \left(\sqrt{\kappa_0} - \frac{\sqrt{6\pi}}{8} \frac{\gamma_0}{\Gamma} \alpha_0 \ell \right) \ln \left(\frac{\sqrt{\kappa_0}}{\sqrt{\kappa_0} - \frac{\sqrt{6\pi}}{8} \frac{\gamma_0}{\Gamma} \alpha_0 \ell} \right) \\ &= \frac{g\mu\omega}{\hbar c} \frac{\sqrt{3}}{2} \sqrt{\frac{At}{\gamma}} \frac{\gamma_0}{\Gamma} \alpha_0 \ell (p-1) \ln \left(\frac{p}{p-1} \right), \end{aligned} \quad (26)$$

with the change of variables

$$\kappa_0 = \frac{3\pi}{64} \left(p \frac{\gamma_0}{\Gamma} \alpha_0 \ell \right)^2. \quad (27)$$

The factor

$$(p-1) \ln \left(\frac{p}{p-1} \right)$$

goes to unity as p goes to infinity; it is approximately 0.9 at $p = 5$. (Further gain from increased power is minimal, and if the power becomes too high, the approximation of the Doppler width being much larger than the power-broadened width breaks down.) Thus, in this case,

$$\begin{aligned} (\delta B)_{DB}^{-1} &\approx 0.8 \frac{g\mu\omega}{\hbar c} \sqrt{\frac{At}{\gamma}} \frac{\gamma_0}{\Gamma} \alpha_0 \ell \\ &\approx 0.3 \frac{g\mu}{\hbar} \lambda \ell n \frac{\gamma_0}{\Gamma} \sqrt{\frac{At}{\gamma}}, \end{aligned} \quad (28)$$

for sufficiently high κ_0 .

This result, where sensitivity increases linearly with optical thickness, holds for the case where the power-broadened width $\sim \gamma_0 \sqrt{\kappa(x)}$ is smaller than the Doppler width for all x within the sample, i.e.

$$\begin{aligned} 1 &\ll \kappa_0 \ll (\Gamma/\gamma_0)^2 \text{ and} \\ \Gamma/\gamma_0 &\ll \alpha_0 \ell \ll (\Gamma/\gamma_0)^2, \end{aligned} \quad (29)$$

since $\alpha_0 \ell$ is related to κ_0 by Eq. (27). As power and optical thickness are increased beyond this range, i.e.

$$\begin{aligned} \kappa_0 &\gg (\Gamma/\gamma_0)^2 \text{ and} \\ \alpha_0 \ell &\gg (\Gamma/\gamma_0)^2, \end{aligned} \quad (30)$$

we obtain the Doppler-free case, where sensitivity increases as the square root of the thickness [Eq. (18)].

V. THE GENERAL CASE

A numerical result can be obtained for the general case where the restrictions (29,30) on κ and $\alpha_0 \ell$ are removed. In a typical experiment, light power is ~ 1 mW, the laser beam diameter is ~ 0.1 cm, $\lambda \approx 800$ nm, and $\Gamma/\gamma_0 \approx 60$. Thus the effective ground state relaxation rate due to the transit of atoms through the laser beam is $\gamma \approx 2\pi \cdot 50$ kHz and the initial saturation parameter is $\kappa_0 \approx 4 \times 10^3$. Here, as in a typical experimental procedure, the optical depth is varied (by changing atomic density) while the laser power is kept constant. Normalized transmission, differential small-field rotation, total small-field rotation, and magnetometric sensitivity are plotted in Fig. 3 as a function of optical depth. For small optical depth, $\kappa > (\Gamma/\gamma_0)^2$ and the medium is effectively Doppler-free. Transmission ($\propto \kappa$) falls linearly until the transition to the Doppler-broadened case is made (dashed line). Then

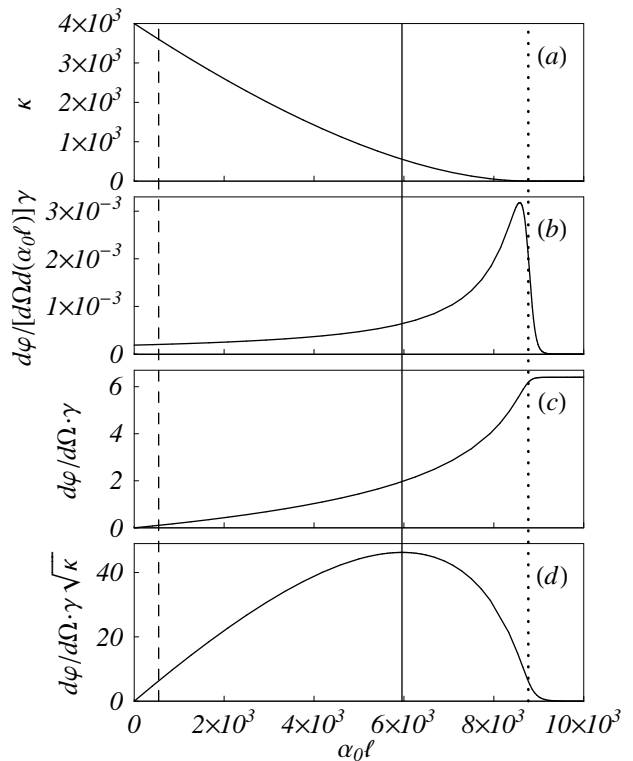


FIG. 3: Normalized (a) saturation parameter, (b) differential small-field rotation, (c) total small-field rotation, and (d) inverse magnetometric sensitivity as a function of optical depth with initial saturation parameter $\kappa_0 = 4 \times 10^3$ and $\Gamma/\gamma_0 = 60$. Plots (b), (c), and (d) are in units of radians. The dashed line indicates the transition from the Doppler-free to the Doppler-broadened regime [$\kappa = (\Gamma/\gamma_0)^2$], and the dotted line indicates the point at which non-linear effects begin to turn off ($\kappa = 1$). Linear optical rotation is neglected in this plot. The solid line indicates the optical depth at which maximum sensitivity is achieved.

transmission falls quadratically until the linear regime is reached (dotted line), after which it falls exponentially. Differential small-field rotation ($\propto d\varphi/[d\Omega d(\alpha_0 \ell)]\gamma$) initially rises, as κ falls and power broadening is reduced, until non-linear effects begin to turn off. (Linear optical rotation is neglected in this plot.) Since magnetometric sensitivity depends both on total optical rotation and transmission, an intermediate value for the optical depth produces the greatest sensitivity (solid line). Multiplying the normalized inverse sensitivity $d\varphi/d\Omega \cdot \gamma \sqrt{\kappa}$ by

$$2\sqrt{2\pi} \frac{g\mu}{\hbar} \frac{\sqrt{A}}{\lambda\sqrt{\gamma}} \approx 10^8 \left(G/\sqrt{\text{Hz}} \right)^{-1} \quad (31)$$

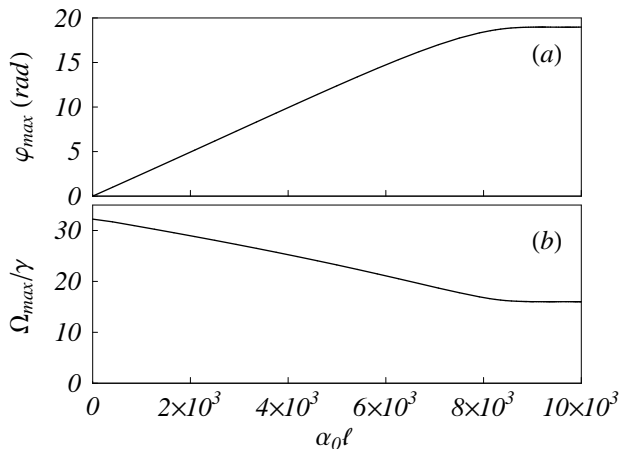


FIG. 4: (a) Maximum optical rotation and (b) normalized magnetic field at which rotation is maximum as a function of optical depth. Parameters are the same as those used for Fig. 3.

gives the absolute magnitude of sensitivity, $\sim 2 \times 10^{-10}$ G/ $\sqrt{\text{Hz}}$ (we assume $g = 1$). Although this sensitivity is not as high as could be achieved with low atomic density paraffin-coated cells ($\sim 3 \times 10^{-12}$ G/ $\sqrt{\text{Hz}}$ [3]), it is, nevertheless, sufficiently high to be of interest in practical applications [10]. In particular, the power-broadening of the magnetic field dependence of optical rotation at high light power provides an increased dynamic range for magnetometry over the low-power case. There are, however, techniques for shifting the narrow resonance obtained with a paraffin-coated cell to higher magnetic fields, e.g., frequency modulation of the laser light [20].

VI. LARGE-FIELD OPTICAL ROTATION

The maximum optical rotation with respect to magnetic field can be determined with a numerical calcula-

tion. Maximum rotation is plotted as a function of optical depth in Fig. 4, for the same parameters as used for Fig. 3. The rotation initially rises linearly, the same behavior seen in the experiment [8] mentioned in the introduction. For large optical depth, however, rotation in Fig. 4 then begins to rise more quickly, and finally saturates, whereas experimentally a slower increase and then a decrease in rotation is seen. This is evidence for an additional relaxation mechanism not accounted for in the present theory; in Ref. [8] it is attributed to the effect of radiation trapping.

VII. CONCLUSION

In conclusion, we have analyzed magnetometric sensitivity of NMOR measurements optimized with respect to light intensity in the case of negligible Doppler broadening, and in the case of large Doppler broadening. In the former case, we find that the sensitivity improves as the square root of optical density, while in the latter, it improves linearly. In the present discussion, we have neglected the effect of velocity-changing collisions, which makes this analysis not directly applicable to buffer-gas and anti-relaxation-coated cells. However, since there is full mixing between velocity components in these cells, one can expect that the sensitivity should scale as square root of optical density (if this quantity can be varied independently of the ground state relaxation rate).

The authors are grateful to D. F. Kimball, I. Novikova, V. V. Yashchuk, and M. Zolotarev for helpful discussions. This work has been supported by the Office of Naval Research (grant N00014-97-1-0214).

-
- [1] W. Gawlik, in *Modern Nonlinear Optics*, edited by M. Evans and S. Kielich (Wiley, New York, 1994), vol. LXXXV of *Advances in Chemical Physics*, p. 733.
- [2] D. Budker, D. J. Orlando, and V. Yashchuk, *Am. J. Phys.* **67**(7), 584 (1999).
- [3] D. Budker, D. F. Kimball, S. M. Rochester, V. V. Yashchuk, and M. Zolotarev, *Phys. Rev. A* **62**(4), 043403/1 (2000).
- [4] S. E. Harris, *Phys. Today* **50**(7), 36 (1997).
- [5] M. O. Scully and M. Fleischhauer, *Phys. Rev. Lett.* **69**(9), 1360 (1992).
- [6] M. Fleischhauer and M. O. Scully, *Phys. Rev. A* **49**(3), 1973 (1994).
- [7] V. A. Sautenkov, M. D. Lukin, C. J. Bednar, I. Novikova, E. Mikhailov, M. Fleischhauer, V. L. Velichansky, G. R. Welch, and M. O. Scully, *Phys. Rev. A* **62**(2), 023810/1 (2000).
- [8] I. Novikova, A. B. Matsko, and G. R. Welch, *Opt. Lett.* **26**(13), 1016 (2001).
- [9] A. B. Matsko, I. Novikova, M. O. Scully, and G. R. Welch, *Phys. Rev. Lett.* **87**(13), 133601/1 (2001).
- [10] I. Novikova and G. R. Welch, *J. Mod. Opt.* **49**, 349 (2002).
- [11] A. B. Matsko, I. Novikova, and G. R. Welch, *J. Mod. Opt.* **49**, 367 (2002).
- [12] M. Fleischhauer, A. B. Matsko, and M. O. Scully, *Phys. Rev. A* **62**(1), 013808/1 (2000).
- [13] D. Budker, D. F. Kimball, S. M. Rochester, and V. V. Yashchuk, *Phys. Rev. Lett.* **85**(10), 2088 (2000).
- [14] S. Stenholm, *Foundations of laser spectroscopy*, Wiley

- series in pure and applied optics (Wiley, New York, 1984).
- [15] S. M. Rautian and A. M. Shalagin, *Kinetic problems of non-linear spectroscopy* (North-Holland, Amsterdam, 1991).
- [16] S. Huard, *Polarization of light* (Wiley, New York, 1997).
- [17] S. M. Rochester, D. S. Hsiung, D. Budker, R. Y. Chiao, D. F. Kimball, and V. V. Yashchuk, Phys. Rev. A **63**(4), 043814/1 (2001).
- [18] I. B. Khriplovich and S. K. Lamoreaux, *CP violation without strangeness : electric dipole moments of particles, atoms, and molecules*, Texts and monographs in physics (Springer-Verlag, Berlin, 1997).
- [19] W. Demtröder, *Laser spectroscopy : basic concepts and instrumentation* (Springer, Berlin, 1996), 2nd ed.
- [20] D. Budker, D. F. Kimball, V. V. Yashchuk, and M. Zolotarev, Submitted (2002).
- [21] D. Ulam-Orgikh and M. Kitagawa, Phys. Rev. A **64**(5), 052106/1 (2001).
- [22] In the general case, there may exist an additional source of noise due to AC-Stark shift associated with off-resonant levels [12]; however, this source of noise is absent for an isolated transition such as the one considered here.
- [23] The use of so-called spin-squeezed quantum states of light (see, e.g., Ref. [21] and references therein) can, in principle, allow one to overcome the SQL. We consider only non-squeezed states of atoms and light here.